JVI Accepted Manuscript Posted Online 28 June 2017
J. Virol. doi:10.1128/JVI.00838-17

Inhibition of Poxvirus Gene Expression and Genome Replication by Bisbenzimide Derivatives

Artur Yakimovich[1,3,6], Moona Huttunen[3,6], Benno Zehnder[2], Lesley J Coulter[4], Victoria Gould[3], Christoph Schneider[5], Manfred Kopf[5], Colin J McInnes[4], Urs F. Greber[1*], Jason Mercer[2,3*]

1 Institute of Molecular Sciences, University of Zurich

2 Institute of Biochemistry, ETH Zurich

3 MRC Laboratory for Molecular Cell Biology, University College London

4 Moredun Research Institute, Pentlands Science Park, Bush Loan, Penicuik, EH26 0PZ

5 Institute of Molecular Health Sciences, Department of Biology, ETH Zurich

6 These authors contributed equally to this work

*Correspondence: urs.greber@imls.uzh.ch (U.F.G); jason.mercer@ucl.ac.uk (J.M)

Abstract

Virus infection of humans and livestock can be devastating for individuals and populations, sometimes resulting in large economic and societal impact. Prevention of virus disease by vaccination or anti-viral agents is difficult to achieve. A notable exception was the eradication of human smallpox by vaccination over 30 years ago. Today, humans and animals remain susceptible to poxvirus infections, including zoonotic poxvirus transmission. Here we identified a small molecule, bisbenzimide (bisbenzimidazole) and its derivatives, as potent agents against prototypic poxvirus infection in cell culture. We show that bisbenzimide derivatives, which preferentially bind the minor groove of double stranded DNA, inhibit vaccinia virus infection by blocking viral DNA replication and abrogating post-replicative intermediate and late gene transcription. The bisbenzimide derivatives are potent against vaccinia virus and other poxviruses but ineffective against a range of other DNA and RNA viruses. The bisbenzimide derivatives are the first inhibitors of-their-class, which appear to directly target the viral genome without affecting cell viability.

42

43

44 **Importance**

45 Smallpox was one of the most devastating diseases in human history until it was
46 eradicated by a worldwide vaccination campaign. Due to discontinuation of routine
47 vaccination more than 30 years ago, the majority of today's human population remains
48 susceptible to infection with poxviruses. Here we present a family of bisbenzimide
49 (bisbenzimidazole) derivatives, known as Hoechst nuclear stains, with high potency against
50 poxvirus infection. Results from a variety of assays used to dissect the poxvirus lifecycle
51 demonstrate that bisbenzimides inhibit viral gene expression and genome replication.
52 These findings can lead to the development of novel antiviral drugs that target viral
53 genomes and blocking viral replication.

Introduction

Viral infections are difficult to treat and prevent. Underlying technical reasons, such as diagnosis and viral persistence, viruses occur in large numbers, are genetically adaptable to environmental pressure, and highly dependent on their hosts (1-3). This makes it challenging to treat virus infections with compounds that target viral factors such as enzymes or structural proteins. Compounds directed against host factors required for infection potentially endanger the host, although there is emerging evidence that clinically approved anti-cancer agents have significant efficacy against viruses in post-exposure regimens (4).

Today's world population has become susceptible to poxvirus infection anew, after the discontinuation of smallpox vaccination over 30 years ago. Notable poxvirus cases include variola virus, the causative agent of smallpox, which despite eradication is ranked as a "category A pathogen" by the US National Institute of Allergy and Infectious Diseases. Further agents include vaccinia virus Cantalago and cowpox viruses which are contracted from infected animals and can cause fever and lesions (5-9), and monkeypox, which has a mortality rate estimated around 10% (10) and was responsible for the 2003 poxvirus outbreak in the U.S. (11, 12).

There are few current treatment options against orthopoxvirus infections. These include live attenuated vaccinia virus (VACV)-based vaccines, Dryvax and ACAM2000, which can have some adverse effects including fever, rash, encephalitis and in rare cases (1:1,000,000) death (13, 14). Small molecule compounds against orthopoxvirus infections include Cidofovir, a nucleotide analog targeting the viral DNA polymerase (15), and ST-246 (tecovirimat, TPOXX), the most promising anti-poxvirus drug, that inhibits virus cell-to-cell spread (16-18). For both Cidofovir and ST-246, poxvirus resistance has been reported (16,

19, 20). Remarkably, a single point mutation within the viral genome is sufficient to give rise to ST-246-resistance (16). In the face of a limited number of anti-poxvirus drugs there is an obvious need for novel antivirals directed against poxviruses.

Targeting of the viral replication machinery by antivirals has been successfully employed against RNA and DNA viruses (15, 21-24). Inhibition of viral polymerases and helicases is effective as this strategy leads to sustained inhibition of genome replication thereby slowing the emergence of drug resistant mutations. To date, direct targeting of viral genomes by anti-viral agents has not been reported.

Bisbenzimides are a class of fluorescent dyes that bind within the minor groove of double stranded DNA (dsDNA) preferentially to AT rich regions (25-29). These compounds have been used to drive pro-apoptotic and cytostatic activity in cancer cells (30, 31). In addition, bisbenzimide derivatives have been reported to indirectly modulate mammalian and bacterial topoisomerase I and II activity (32-35). Yet their application as antiviral agents has not been explored.

Here, we present evidence that a set of bisbenzimide derivatives, which are commonly known as Hoechst compounds (29, 36-38), display potent anti-poxvirus activity far separated from cell toxicity. Dissection of poxvirus temporal gene expression, uncoating, genome replication and virus yield indicates that bisbenzimide-mediated anti-poxvirus activity occurs through inhibition of viral intermediate and late gene transcription as well as genome replication.

Results

Bisbenzimides inhibit VACV infection

To determine if bisbenzimides have antiviral activity against VACV we tested the ability of three different bisbenzimides to inhibit viral plaque formation assays, Hoechst 33342 (H4), Hoechst 33258 (H5), and Hoechst 34580 (H8) (Fig. 1A). Confluent monolayers of green monkey kidney (BSC40) cells were infected with serial dilutions of VACV strain Western Reserve (WR) which expresses EGFP from an early/late promoter (WR E/L EGFP) in the presence or absence of H4, H5 or H8. A known inhibitor of VACV DNA replication, cytosine arabinoside (AraC) (39, 40), served as a positive control in these experiments. At 24 h post infection (hpi) plates were imaged for nuclei indicating cell numbers, and GFP expression, a surrogate for infection (Fig. 1B). The total cell number and the number of infected cells were quantified using Plaque 2.0 (41) (Fig. 2). The H compounds displayed no apparent cell toxicity, with the exception of H4, and to a low extent H8 at the highest concentration tested of 20 µM. With each H compound, dose dependent inhibition of VACV infection was observed. H4 was the most potent compound, causing a complete block of VACV infection at 2µM regardless of virus concentration. H5 and H8 were less effective, both reaching complete inhibition at 20µM (Fig. 2). These effects were not specific to BSC40 cells, since similar results were obtained in L929 mouse fibroblasts (data not shown). The data show that bisbenzimides H4, H5, and H8 exert potent inhibitory activity against VACV infection with little cell toxicity when used at low µM concentrations.

Bisbenzimides block intermediate and late but not early viral gene expression

We next tested the impact of the most potent early/late gene expression inhibitor (H4) and the least toxic compound (H5) on early and late viral gene expression. VACV gene

123 expression occurs in three temporal stages, early, intermediate, and late. Early gene
124 expression (EGE) occurs prior to DNA replication while intermediate gene expression (IGE)
125 and late gene expression (LGE) requires DNA replication.

126 BSC40 or HeLa cells were pretreated with H4 or H5 and infected with recombinant VACVs
127 encoding EGFP under the control of an early (WR E EGFP) or a late (WR L EGFP) viral
128 promoter. Cells treated with cycloheximide (CHX) and AraC served as positive controls for
129 inhibition of EGE and LGE, respectively (Fig. 3). Infection was quantified by flow cytometry
130 8 hpi. In BSC40 cells H4-treatment inhibited EGE up to 42% at 20µM, and completely
131 blocked LGE at 800nM and above. H5 on the other hand did not inhibit EGE at any of the
132 tested concentrations, but showed a dose-dependent inhibition of LGE of up to 90% from
133 2µM to 20µM (Fig. 3A). In HeLa cells the trend of inhibition by H4 and H5 was similar but
134 the compounds were more potent than in BSC40 cells with H4 resulting in complete
135 inhibition of EGE at 4µM and LGE at 200nM, and H5 showing no impact on EGE, but
136 inhibiting LGE by 100% at 4µM (Fig. 3B).

137 The half maximum (EC_{50}) and maximum (EC_{90}) effective concentration for inhibition of
138 EGE, IGE, and LGE were determined for H4 (Fig. 3C). HeLa cells were pre-treated with
139 various concentrations of H4 and infected with WR E EGFP, WR I EGFP, or WR L EGFP
140 viruses. Consistent with the date in Figure 2, the EC_{50} of H4 for EGE was 800nM and the
141 EC_{90} 1.6µM (Fig. 3C; blue line). H4 was even more effective against IGE and LGE with
142 EC_{50} inhibition of IGE or LGE at 20nM, and EC_{90} at 80nM (Fig. 3C; green and red lines).
143 These results show that the bisbenzimide H4 is an effective inhibitor of VACV IGE and
144 LGE at nM concentrations.

145 **H4 blocks VACV plaque formation and reduces viral yield**

146 Given the potent effect of H4 on IGE and LGE, we next assessed the ability of H4 to inhibit
147 plaque formation and produce progeny. For plaque formation, monolayers of HeLa cells
148 were infected with 150 plaque forming units (pfu) of VACV in the absence (NoT) or
149 presence of 20nM or 80nM H4. At 72 hpi monolayers were assessed for plaque formation
150 by staining the residual cells with crystal violet (Fig. 4A). In the presence of 20nM H4 both
151 the size and number of plaques were strongly reduced, with a few small plaques detected.
152 At 80nM H4 no visible plaques were visible.

153 Next we assessed the impact of H4 on virus production in HeLa cells. In the presence of
154 20nM H4 the number of infectious particles was reduced by 1.5 logs at 24 hpi. In the
155 presence of 80nM H4, virus production was reduced by 4 logs relative to the 24 h yield in
156 untreated cells (Fig. 4B). The results show that H4 effectively blocked VACV plaque
157 formation and the production of infectious particles, even over extended periods (72 h) of
158 incubation.

159 **H4 targets an early stage of VACV infection**

160 To address the stage of the virus lifecycle blocked by H4 we conducted add-in or wash-out
161 experiments with H4 at different times of infection. When 80nM H4 was added as early as
162 6 hpi, virus yield was reduced by ≥90% compared to no drug treated cells (Fig. 4C).
163 Addition of H4 at 9 hpi gave a 50% reduction, and addition at 12 hpi had no impact on virus
164 yield (Fig. 4C). In wash-out experiments only early washout of H4, for example at 30 or 90
165 min pi, partially rescued virus yield, whereas washout at later times essentially had no
166 rescue effects (Fig. 4D). These results indicated that H4 is most effective during early
167 stages of infection.

168 **Pretreatment of purified VACV virions with H4 does not impact infectivity**

169 Remarkably H4 had little impact on EGE but diminished virus yield at early infection times
170 when events such as EGE occur. To resolve this puzzling notion, we tested if H4 directly
171 affected the infectivity of virions. WR E EGFP and WR L EGFP viruses were pre-incubated
172 with H4 at 20nM (EC_{50}) or 80nM (EC_{90}), extensively washed to remove residual
173 bisbenzimide, and added to HeLa cells. Cells were harvested and infection was analyzed
174 by flow cytometry 8 hpi (Fig. 4E). Results showed that pre-incubation of virions with H4 had
175 no significant impact on either EGE or LGE. To confirm these results a range of WR E/L
176 EGFP virus concentrations were pre-incubated for various times with 2µM H4, a
177 concentration which completely blocked EGE and LGE in HeLa cells (see Fig. 3B and C).
178 Untreated and pre-treated virions were washed extensively before addition to cells. After
179 24 h, infection was quantified using the microscopy-based Plaque2.0 assay (Fig. 4F). As
180 expected infection was dose-dependent, yet even at 2µM H4, no inhibition of VACV
181 infection was observed. These results show that H4 does not directly impact the infectivity
182 of extracellular virions but rather acts on a critical intracellular stage of the VACV lifecycle.

183 **H4 treatment does not impact VACV genome uncoating**

184 Given that H4 had no impact on EGE but effectively blocked IGE and LGE we assessed
185 genome uncoating [reviewed in (42, 43)], as it is a pre-requisite for VACV genome
186 replication and subsequent IGE and LGE. Incoming VACV genomes released into the
187 cytoplasm, termed pre-replication sites, can be visualized by immunofluorescence directed
188 against the viral single-stranded DNA binding protein I3, or with click-chemistry based
189 detection of single virus genomes (44-48).

190 Here we used I3 staining to test the influence of H4 on VACV pre-replication site formation,
191 HeLa cells were infected in the presence of 20nM, 80nM or 200nM H4, fixed at 5 hpi and
192 stained for I3 (Fig. 5A). AraC, which blocks viral replication post uncoating, and CHX,

193 which blocks uncoating by inhibiting the synthesis of the VACV uncoating factor (47) were
194 included as controls. As expected CHX prevented the formation of pre-replication sites,
195 while AraC did not affect the number of I3 puncta. H4 did not affect the number of I3-
196 positive pre-replication sites (Fig. 5B). These results show that H4 does not affect VACV
197 genome uncoating even at concentrations above those that inhibit IGE and LGE.

198 **High concentrations of H4 inhibit VACV DNA replication**

199 We next tested the impact of H4 on VACV DNA replication site formation. Cells were
200 infected in the presence of 20nM, 80nM, or 200nM H4 and assessed for replication site
201 formation by staining with 4',6-diamidino-2-phenylindole (DAPI) at 8 hpi. As expected,
202 untreated cells contained large cytoplasmic VACV replication sites while AraC treated cells
203 had none (Fig. 6A). The replication sites in H4- treated cells showed phenotypic differences
204 from control infections. At 20nM the replication sites appeared slightly smaller and more
205 diffuse, and at 80nM and 200nM the size of the replication sites was reduced and many
206 small DAPI positive puncta were seen (Fig. 6A). When the number of cells containing
207 replication sites was quantified, without accounting for their size or number, treatment with
208 20nM or 80nM H4 showed a 14.9 % and 20.7 % decrease respectively, while treatment
209 with 200nM H4 decreased cells containing replication sites by 48.2 % (Fig. 6B). We noticed
210 that the replication sites seen in the presence of 200nM H4 were larger than the pre-
211 replication sites seen in the presence of AraC (Fig. 5A). This suggested that H4 did not
212 block DNA replication initiation, but rather acted after the onset of replication.

213 To assess the impact of H4 on on-going replication we used 5-ethynyl-20-deoxyuridine
214 (EdU) and click chemistry labeling (48). Cells were infected in the absence or presence of
215 20nM, 80nM, or 200nM H4 and the incorporation of EdU into viral replication sites was
216 assessed at 8 hpi (Fig. 6C). Untreated cells displayed numerous bright EdU-positive

replication sites. At 20nM and 80nM the replication sites appeared less numerous but brighter, while at 200nM small replication sites with little EdU incorporation were seen (Fig. 6C). Quantification of the intensity of EdU/cell confirmed that nucleoside incorporation into viral replication sites was slightly reduced at 20nM and 80nM H4, and strongly reduced in the presence of 200nM H4 to the levels seen in the presence of AraC (Fig. 6D).

H4 blocks VACV DNA replication, IGE and LGE in a dose dependent fashion

Given the considerable size of the viral replication sites seen in the presence of 20nM and 80nM H4, we performed qPCR to quantify VACV DNA synthesis in the presence of H4 (49). Total DNA was extracted from cells infected with VACV at 8 hpi, and the amount of viral DNA quantified. While AraC blocked DNA accumulation as expected, no defect in viral DNA content was seen in the presence of 20nM H4, and a modest decrease of 11% was observed at 80nM H4 (Fig. 6E). VACV DNA accumulation was reduced by 88% in the presence of 200nM H4, consistent with the small replication site phenotype observed in Figure 6.

As VACV IGE and LGE occur after DNA replication it was surprising to find that DNA accumulation was largely unimpeded in the presence of 20nM and 80nM H4, the respective EC_{50} and EC_{90} against VACV infection. We reasoned that H4 may be inhibiting transcription of VACV IGE and LGE at these low concentrations. Using quantitative reverse transcription PCR (RT-qPCR) we assessed the impact of H4 on the accumulation of viral early (J2), intermediate (G8), and late (F17) mRNAs (Fig. 6F). While H4 had little impact on early viral mRNA amounts, accumulation of intermediate mRNA was diminished by 72% and late by 48% at 20nM H4 (Fig. 6F). At 80nM and 200nM H4, intermediate mRNA accumulation was completely abrogated and late mRNA reduced by 88% and 76%, respectively. These results indicate that the bisbenzimide H4 impedes VACV infection by

241 inhibiting two stages of the virus lifecycle; at low levels (20nM and 80nM), H4 inhibits IG
242 and LG transcription, and at elevated levels (200nM), it inhibits VACV DNA replication as
243 well as IG and LG transcription.

244 **Poxvirus infection is acutely sensitive to the antiviral activity of H4**

245 Given the potent inhibitory effects of H4 on VACV transcription and replication we asked if
246 H4 could inhibit infection by other poxviruses. We tested three different parapoxviruses:
247 ORF-11, MRI-SCAB (50), and squirrelpox virus (SQPV) (51). For this, Foetal Lamb Skin
248 cell monolayers were infected with these viruses in the presence of 20nM, 80nM, or 200nM
249 H4. Cell monolayers were assessed for plaque formation at 3 days PI with VACV or ORF-
250 11, and 7 days with MRI-SCAB or SQPV. In the absence of H4 all viruses produced
251 plaques, or in the case of SQPV destroyed the monolayer (Fig. 7A). Strikingly, treatment
252 with H4 at 20nM, 80nM, or 200nM completely attenuated plaque formation by all the
253 viruses (Fig. 7A). These results demonstrate that the bisbenzimides H4 is a broad range
254 inhibitor of poxvirus infection across different genera.

255 While we had shown previously that H4 did not affect plaque formation by human
256 adenovirus (52), we wanted to test the impact of H4 on other viruses, Herpes simplex
257 virus-1 (HSV) which replicates in the nucleus (53), and RNA viruses which replicate either
258 in the nucleus (Influenza A virus, IAV), or the cytoplasm (Vesicular Stomatitis Virus, VSV;
259 Semliki Forest Virus, SFV). When cells were infected with these viruses in the presence of
260 20nM or 200nM H4, expression of GFP from reporter viruses was not significantly
261 impacted regardless of the concentration used (Fig. 7B). We conclude that bisbenzimides
262 are rather selective inhibitors against poxviruses and do not affect a broad range of
263 unrelated viruses.

Discussion

Bisbenzimides are a class of fluorescent dyes commonly used in flow cytometry and fluorescence microscopy to identify cell nuclei. Bisbenzimides stain DNA in the nucleus and cytoplasmic organelles, such as mitochondria and chloroplasts (36). Here we demonstrate that a range of bisbenzimides are potent inhibitors of poxvirus infection. We used a variety of virological assays to determine the stage of the VACV lifecycle impacted by H4, the most effective H derivative tested. We found that H4 did not inhibit infection by acting on extracellular viral particles, nor by targeting the early stages of the virus lifecycle, including EGE and DNA uncoating. Analysis of viral EG, IG, and LG transcription, DNA replication site formation, and viral DNA synthesis indicated that H4 blocked IG and LG transcription as well as DNA replication in a dose-dependent manner. H4 strongly inhibited the production of infectious VACV particles, and plaque formation was impeded in its presence.

Our results indicate that the effectiveness of bisbenzimides against poxviruses correlates with the accessibility of the viral DNA to solutes. We found that the H compounds did not affect the infectivity of VACV particles when the particles were intact, that is when they were outside of cells. The compounds were effective after viral DNA was released from the capsid into the cytosol, where it is replicated. Consistent with this, the EC_{50} of H4 against EGE, which occurs when the viral core is largely intact, was 20-fold higher than the EC_{50} for IGE and LGE, which only occurs from exposed viral DNA. EG transcription occurs within cytoplasmic viral cores prior to genome uncoating, while IG and LG transcription occur in the cytoplasm after viral genome replication (54). High concentrations of H4 could impact early gene expression during the activation of cytosolic cores, which expand when EG transcription [(55-57) and (58)]. We speculate that core expansion may lead to

increased accessibility of the VACV genomes within. That early, intermediate, and late VACV mRNAs are all translated in the cytoplasm on host ribosomes makes it unlikely that bisbenzimides impact translation of viral proteins.

We noted that the inhibitory efficacy of the bisbenzimides correlated with their lipophilicity, H4>H8>H5 (Fig. 1A). Lipophilicity largely dictates the binding of bisbenzimides to double-stranded DNA via hydrophobic interactions with adenosine-threonine (A=T) rich regions (25, 59, 60). Since poxviruses with differential genomic A=T content, that is VACV (67% A=T), ORFV (36% A=T), and SQPV (33% A=T) (61), display similar sensitivity to H4 it is unlikely that poxviruses are susceptible to bisbenzimides simply due to their high A=T content. It is more likely that the solute accessibility of the viral genome and the association of DNA binding proteins dictates susceptibility of the virus to the H compounds.

Remarkably, despite their effectiveness against poxviruses the H-bisbenzimides tested had no effect on infection by other DNA viruses, such as adenovirus or herpesvirus. As opposed to poxviruses, herpesviruses and adenoviruses deliver their infectious incoming DNA genomes directly into the nucleus where they are transcribed and replicated (48, 53, 62-64). It is possible that bisbenzimides do not efficiently bind to the nuclear DNA of adenovirus and herpes virus due to the spatial proximity of host DNA, which acts as an efficient local avidity trap for the bisbenzimides. In this scenario, bisbenzimides used at low nanomolar, non-toxic concentrations would be more likely to bind to host DNA than viral DNA.

While selection of VACV variants resistant to the anti-poxvirus agents cidofovir or ST-246 is readily possible (16, 65), we were unable to isolate a bisbenzimide-resistant VACV in up to 20 passages at different concentrations of H4 (data not shown). This is consistent with our finding that H4 targets at least two viral processes. Low concentrations of H4 inhibited

IG and LG transcription, while higher concentrations of H4 also blocked viral DNA replication. IG and LG transcription inhibition at low H4 concentrations could occur since the intermediate and late promoters are AT-rich (66), and H4 preferentially binds to AT-rich dsDNA. The presence of small highly condensed viral DNA replication sites observed in the presence of high concentrations of H4, and the observation that VACV topoisomerase DNA unwinding activity is unaffected *in vitro* (data not shown) (67), suggests a model in which bisbenzimides block DNA replication by coating cytoplasmic VACV genomes.

In sum, we show that bisbenzimide compounds are highly specific for inhibiting poxvirus infections at low apparent cytotoxicity. It is possible that the bisbenzimides tested here are also effective against divergent members of the nucleocytoplasmic large DNA viruses that replicate exclusively in the cytoplasm (68). Bisbenzimide compounds have been used in mice with potential antitumor effects (30), and were tested in a phase I-II advanced pancreatic carcinoma study in humans (69). Notably, in both cases bisbenzimides were well tolerated. While the *in vivo* efficacy of bisbenzimides against poxvirus infection has not been determined, the dual mechanism of inhibition, that is intermediate / late gene expression and viral DNA replication, appears to be a high barrier against the emergence of viral resistance. This makes it tempting to speculate that bisbenzimides may serve as attractive anti-poxvirus drugs, either alone or in combination with CMX001 and ST-246 (70).

Materials and Methods

Cell Culture and Reagents

All cells lines used were cultivated as monolayers at 37.0 °C and 5.0% CO2. Cells were cultured in Dulbecco's Modified Eagle Medium (DMEM, GIBCO, Life Technologies,

335 Switzerland). HeLa (ATCC) and mouse subcutaneous areolar and adipose cells L929
336 (ATCC) were cultivated in DMEM with the addition of 10% Fetal Bovine Serum (FBS,
337 Sigma), 2mM GlutaMAX (Life Technologies) and 1% peneciline-streptomycine (Pen-Strep,
338 Sigma). Cercopithecus aethiops kidney epithelial cells (BSC40, ATCC) were cultivated in
339 DMEM with 10% FBS, 2mM GlutaMAX, 1% Non-essential amino acids mix (NEAA, Sigma)
340 and 1mM sodium pyruvate (NaPyr, Sigma). HDFn human foreskin fibroblasts cell line
341 (Invitrogen) was cultivated in DMEM containing 5% FBS. Foetal Lamb Skin cells were
342 cultivated in Media 199 (Sigma) with 2 % glutamine, 0.16 % sodium hydrogen carbonate,
343 10 % tryptose phosphate broth, and 10 % FBS.

344 **VACV and Parapoxvirus Strains and Virus Purification**

345 Vaccinia virus strain Western Reserve (VACV WR) (71) and International Health
346 Department J (VACV IHD-J) (72) were used throughout. These strains were either wild
347 type (WT) or transgenic containing early/late EGFP (E/L EGFP VACV WR, E/L EGFP
348 VACV IHD-J), early EGFP (E EGFP VACV WR), intermediate EGFP (I EGFP VACV WR),
349 late EGFP (L EGFP VACV WR). All VACV mature virions (MVs) were purified from
350 cytoplasmic lysates by pelleting through a 36% sucrose cushion for 90 min at 18,000 x g.
351 The virus pellet was resuspended in 10mM Tris pH 9.0 and subsequently banded on a 25
352 to 40% sucrose gradient at 14,000 x g for 45 min. Following centrifugation, the viral band
353 was collected by aspiration and concentrated by pelleting at 14,000 x g for 45 min. MVs
354 were resuspended in 1mM Tris pH 9.0 and tittered for plaque forming units per milliliter
355 (PFU/ml) as previously described (73). The parapoxvirus strains used include a tissue
356 culture adapted strain, ORF-11, a non-adapted strain MRI-SCAB, and Squirrelpox (SQPV).
357 IAV was obtained from Yohei Yamauchi, SFV and VSV were obtained from Giuseppe
358 Balistreri, HSV-1 was obtained from Cornel Fraefel.

359 **Inhibitors, Dyes, Antibodies and Plasmids**

360 Cycloheximide (CHX, Sigma) was used at 50µM, cytosine arabinosid (Cytarabine, Ara-C,
361 Sigma) was used at 10µM. Bisbenzimides H4, H8 and H5 (Sigma) were dissolved in water
362 and used as described in the respective experiments. Rabbit polyclonal anti-EGFP was
363 used in 1:1000 dilution. Anti-I3 antibody (generous provided by Jakomine Krijnse Locker;
364 Institute Pasteur) was used at 1:500. All secondary antibodies goat anti-rabbit-AF488 and
365 goat anti-rabbit-AF594 (Invitrogen) were used at 1:1000.

366 **Plaque2.0 Assay**

367 BSC40 cells were cultivated as monolayers in 96-well imaging plates (Greiner Bio-One,
368 Germany) and inoculated with a serial dilution of either E/L EGFP VACV WR or E/L EGFP
369 VACV IHD-J. 1 hpi the inoculum was removed and replaced with medium (non-treated
370 control) or a respective dilution of an experimental compound in the medium. 24 hpi plates
371 were fixed with 4% PFA and stained with Hoechst nuclear stain. Plates were imaged using
372 ImageXpress XL Micro epi-fluorescent high-throughput microscope (Molecular Devices,
373 USA) with a 4x air objective (Nikon, Japan) in a tile mode allowing full well reconstruction.
374 Image processing and analysis was performed using Plaque2.0 software (41) . Experiment
375 was performed in three technical replicas (triplicate).

376 **Early, Intermediate and Late VACV Gene Expression Analysis**

377 HeLa or BSC40 cells in 24-well plates were infected with E EGFP VACV WR and L EGFP
378 VACV WR at MOI 5 together with H4 in different concentrations. To quantify EGE or IGE
379 and LGE cells were infected for six or eight hours, respectively. Cells were detached with
380 0.05% Trypsin-EDTA and fixed in 4% formaldehyde for 15 minutes. After centrifugation at
381 500 g for 5 min, the cell pellets were re-suspended in 400 µl FACS buffer. A BD Bioscience

382 FACSCalibur flow cytometer was used for analysis and 10,000 cells per condition were
383 measured.

384 **Virus Titrations by Plaque Assay**

385 Viruses were diluted in the cell line appropriate media and 250µL or 500 µl of this virus
386 dilution added to HeLa or Foetal Lamb Skin cell monolayers in 6-well plates. The plates
387 were rocked every 15 minutes and after 1 hour, media was aspirated and cells fed with full
388 media containing the indicated compound concentrations. The cells were then incubated at
389 37 °C for 3, 4, or 7 days (as indicated) before staining with 0.1% crystal violet in 3.7% PFA.

390 **24 h Virus Yield**

391 HeLa cells in 12-well plates were infected at MOI 1 in presence of the compound. After 24
392 h cells were collected, centrifuged, and the pellet re-suspended in 100µl 1mM Tris pH 9.0.
393 Cells were freeze-thawed three times to lyse the cells and the virus solution subjected to
394 serial titration to determine the pfu/ml.

395 **Add-in and Wash-out Assays**

396 HeLa cells were grown in 12-well plates and infected with WT VACV WR at MOI 1. For
397 wash-out experiments, infection was performed in the presence of 80nM H4. At indicated
398 time point the cells were washed five times with medium and infection allowed to proceed
399 in the absence of compound. For add-in experiments, medium containing 80nM H4 was
400 added to the cells at the indicated time points. For both, at 24 hpi, cells were collected and
401 titered as above.

402 **Pre-treatment of Virus Particles with H4**

Viruses expressing EGFP from early or late promoters were pre-incubated with 20nM or 80nM H4 for the indicated times at room temperature. The virus particles were washed three times in media and used to infect HeLa cells. Similarly, to early and late gene profiling, infection was stopped after 6 to 8 hpi and infection analyzed by flow cytometry.

Pre-replication Site Visualization

HeLa cells were infected with WT VACV at MOI 10 in the presences of AraC and 20nM, 80nM or 200nM H4. At 5 hpi cells were fixed, nuclei stained with Dapi and pre-replication sites visualized by immunofluorescence staining against VACV I3. Images were acquired by confocal microscopy and Max projections generated from 10 Z-stacks. The number of pre-replication sites/cell in the presence of 20nM, 80nM or 200nM H4 was determined by spot detection of the MaxIntProjections with a (Fiji: spots larger than 5 pixels). Cells treated with CHX alone served as controls for genome uncoating and replication site formation, respectively.

Replication Site Formation

HeLa cells were infected with WT VACV at MOI 5 in the presence of 20nM, 80nM or 200nM H4. At 8hpi, cells were fixed and VACV replication sites visualized by staining with Dapi. The percentage of cells containing replication sites were quantified by manual counting due to the shape and size variation of replication sites under the various conditions. AraC sample served as a control for inhibition of DNA replication site formation.

EdU Accumulation

HeLa cells were infected with WT VACV at MOI 10. After 1h virus binding in DMEM, the media was changed to 10% DMEM containing 1μM EdU in the presence of absence of H4

(20 nM, 80 nM, or 200 nM). At 8 hpi cells were fixed with 4% PFA and stained using Click-iT EdU Imaging kit (Thermo Scientific) and Hoechst to visualize cell nuclei. Cells were imaged using confocal microscopy and analyzed using CellProfiler/KNIME software. Briefly, the intensity of EdU staining per sample was determined after background subtraction and exclusion of nuclei by image segmentation.

Viral DNA Quantification by qPCR

HeLa cell monolayers were infected with WR (MOI 10) in the absence or presence of H4 for 8 h. Total DNA was extracted using the Qiagen DNeasy Blood and Tissue Kit according to the manufacturer's instruction. Total DNA concentrations were assessed using a Nanodrop™ spectrophotometer and a portion of total DNA was used in qPCR assay using Mesa Blue qPCR MasterMix Plus for SYBR Assay system (Eurogentec) with following primers: C11R (5'-AAACACACACTGAGAAACAGCATAAA-3' and 5'-ACTATCGGCGAATGATCTGATTA-3'). Concentration of viral DNA was determined by plotting against a standard curve of VACV DNA from purified virions.

Reverse Transcriptase-PCR

HeLa cell monolayers were infected with WR (MOI 10) in the absence or presence of H4 for 2, 4, or 8 h. Total RNA was harvested from infected cells using the Qiagen RNeasy kit according to manufacturer's instructions. Subsequently, 1 µl of total RNA was reverse-transcribed into single-stranded cDNA with SuperScript-II reverse transcriptase (Thermo Fisher Scientific) and oligo(dT) primers. Amplification of J2 (early) from 2 h samples, G8 (intermediate) from 4 h samples, F17 (late) from 8 h samples, and glyceraldehyde-3-phosphate dehydrogenase (GAPDH) cDNA from all time points was performed by qPCR (Mesa Blue qPCR MasterMix Plus for SYBR Assay, Eurogentec) using primers specific for

VACV J2R (5′-TACGGAACGGGACTATGGAC-3′ and 5′-GTTTGCCATACGCTCACAGA-3′), G8R (5'-AATGTAGACTCGACGGATGAGTTA-3', 5'-TCGTCATTATCCATTACGATTCTAGTT-3'), F17R (5'-ATTCTCATTTTGCATCTGCTC-3', 5'-AGCTACATTATCGCGATTAGC-3'), and GAPDH (5' AAGGTCGGAGTCAACGGATTTG GT-3' and 5'-ACAAAGTGGTCGTTGAGGGCAATG-3'). Viral mRNA Ct values are displayed as abundance normalized against GAPDH.

Influenza A Virus, Semliki Forest Virus, Vesicular stomatitis Virus and Herpes Simplex Virus-1 infections

EGFP expressing variants of the indicated viruses were used for these experiments. For each, HeLa cells were infected at an MOI of 5 in the presence of 20nM or 200nM of H4 and cells prepared for flow cytometry analysis between 6 and 8 hpi.

Acknowledgments

We would like to thank Ari Helenius for discussion and support. This work was supported by Jenny and Antti Wihuri Foundation, Finland (to M.H.), the Scottish Government Rural and Environment Science and Analytical Services (RESAS) (to C.J.M. and L.J.C.), Swiss National Science Foundation 310030B_141175 (to C.S. and M.K.), Novartis and the Swiss National Science Foundation 310030B_160316 (to U.F.G.), core funding to the MRC Laboratory for Molecular Cell Biology, University College London and the European Research Council 649101—UbiProPox (to J.M.)

A.Y. and U.F.G. and J.M. conceived the study, A.Y., B.Z., M.H., L.J.C., C.S., M.K., C.J.M, U.F.G., and J.M. designed experiments, A.Y., B.Z., M.H., L.J.C., V.G., C.S., and J.M. carried out experiments, A.Y., B.Z., M.H., C.S., M.K., C.J.M., U.F.G., and J.M. interpreted experiments. All authors contributed to writing the manuscript.

References

1. **Lederberg J.** 2000. Infectious history. Science **288:**287-293.
2. **Greber UF, Bartenschlager R.** 2017. Editorial: An expanded view of viruses. FEMS microbiology reviews **41:**1-4.
3. **Koonin EV, Dolja VV, Krupovic M.** 2015. Origins and evolution of viruses of eukaryotes: the ultimate modularity. Virology **479:**2-25.
4. **Prasad V, Suomalainen M, Hemmi S, Greber UF.** 2017. The cell cycle-dependent kinase Cdk9 is a post-exposure drug target against human adenoviruses. ACS Infectious Diseases.
5. **Santos-Fernandes E, Beltrame CO, Byrd CM, Cardwell KB, Schnellrath LC, Medaglia ML, Hruby DE, Jordan R, Damaso CR.** 2013. Increased susceptibility of Cantagalo virus to the antiviral effect of ST-246(R). Antiviral Res **97:**301-311.
6. **Moussatche N, Damaso CR, McFadden G.** 2008. When good vaccines go wild: Feral Orthopoxvirus in developing countries and beyond. J Infect Dev Ctries **2:**156-173.
7. **Kurth A, Wibbelt G, Gerber HP, Petschaelis A, Pauli G, Nitsche A.** 2008. Rat-to-elephant-to-human transmission of cowpox virus. Emerg Infect Dis **14:**670-671.
8. **Vogel S, Sardy M, Glos K, Korting HC, Ruzicka T, Wollenberg A.** 2012. The Munich outbreak of cutaneous cowpox infection: transmission by infected pet rats. Acta Derm Venereol **92:**126-131.
9. **Duraffour S, Mertens B, Meyer H, van den Oord JJ, Mitera T, Matthys P, Snoeck R, Andrei G.** 2013. Emergence of cowpox: study of the virulence of clinical strains and evaluation of antivirals. PLoS One **8:**e55808.
10. **Di Giulio DB, Eckburg PB.** 2004. Human monkeypox: an emerging zoonosis. Lancet Infect Dis **4:**15-25.
11. **Hutson CL, Lee KN, Abel J, Carroll DS, Montgomery JM, Olson VA, Li Y, Davidson W, Hughes C, Dillon M, Spurlock P, Kazmierczak JJ, Austin C, Miser L, Sorhage FE, Howell J, Davis JP, Reynolds MG, Braden Z, Karem KL, Damon IK, Regnery RL.** 2007. Monkeypox zoonotic associations: insights from laboratory evaluation of animals associated with the multi-state US outbreak. Am J Trop Med Hyg **76:**757-768.
12. **Shchelkunov SN.** 2013. An increasing danger of zoonotic orthopoxvirus infections. PLoS Pathog **9:**e1003756.
13. **Kemper AR, Davis MM, Freed GL.** 2002. Expected adverse events in a mass smallpox vaccination campaign. Eff Clin Pract **5:**84-90.
14. **Belongia EA, Naleway AL.** 2003. Smallpox vaccine: the good, the bad, and the ugly. Clinical medicine & research **1:**87-92.
15. **De Clercq E.** 2002. Cidofovir in the treatment of poxvirus infections. Antiviral research **55:**1-13.
16. **Yang G, Pevear DC, Davies MH, Collett MS, Bailey T, Rippen S, Barone L, Burns C, Rhodes G, Tohan S, Huggins JW, Baker RO, Buller RL, Touchette E, Waller K, Schriewer J, Neyts J, DeClercq E, Jones K, Hruby D, Jordan R.** 2005. An orally bioavailable antipoxvirus compound (ST-246) inhibits extracellular virus formation and protects mice from lethal orthopoxvirus Challenge. J Virol **79:**13139-13149.
17. **Blasco R, Moss B.** 1991. Extracellular vaccinia virus formation and cell-to-cell virus transmission are prevented by deletion of the gene encoding the 37,000-Dalton outer envelope protein. Journal of virology **65:**5910-5920.
18. **Chinsangaram J, Honeychurch KM, Tyavanagimatt SR, Leeds JM, Bolken TC, Jones KF, Jordan R, Marbury T, Ruckle J, Mee-Lee D, Ross E, Lichtenstein I, Pickens M, Corrado M, Clarke JM, Frimm AM, Hruby DE.** 2012. Safety and pharmacokinetics of the anti-orthopoxvirus compound ST-246 following a single daily oral dose for 14 days in human volunteers. Antimicrob Agents Chemother **56:**4900-4905.
19. **Becker MN, Obraztsova M, Kern ER, Quenelle DC, Keith KA, Prichard MN, Luo M, Moyer RW.** 2008. Isolation and characterization of cidofovir resistant vaccinia viruses. Virol J **5:**58.

20. **James SH, Price NB, Hartline CB, Lanier ER, Prichard MN.** 2013. Selection and recombinant phenotyping of a novel CMX001 and cidofovir resistance mutation in human cytomegalovirus. Antimicrob Agents Chemother **57:**3321-3325.
21. **De Gascun CF, Carr MJ.** 2013. Human polyomavirus reactivation: disease pathogenesis and treatment approaches. Clinical and Developmental Immunology **2013**.
22. **Magee WC, Hostetler KY, Evans DH.** 2005. Mechanism of inhibition of vaccinia virus DNA polymerase by cidofovir diphosphate. Antimicrobial agents and chemotherapy **49:**3153-3162.
23. **Bradbury J.** 2002. Orally available cidofovir derivative active against smallpox. The Lancet **359:**1041.
24. **Morris K.** 1998. Short course of AZT halves HIV-1 perinatal transmission. Lancet **351:**651.
25. **Fornander LH, Wu L, Billeter M, Lincoln P, Norden B.** 2013. Minor-groove binding drugs: where is the second Hoechst 33258 molecule? J Phys Chem B **117:**5820-5830.
26. **Han F, Taulier N, Chalikian TV.** 2005. Association of the minor groove binding drug Hoechst 33258 with d(CGCGAATTCGCG)2: volumetric, calorimetric, and spectroscopic characterizations. Biochemistry **44:**9785-9794.
27. **Smith PJ, Lacy M, Debenham PG, Watson JV.** 1988. A mammalian cell mutant with enhanced capacity to dissociate a bis-benzimidazole dye-DNA complex. Carcinogenesis **9:**485-490.
28. **Comings D, Avelino E.** 1975. Mechanisms of chromosome banding. Chromosoma **51:**365-379.
29. **Latt SA, Stetten G.** 1976. Spectral studies on 33258 Hoechst and related bisbenzimidazole dyes useful for fluorescent detection of deoxyribonucleic acid synthesis. J Histochem Cytochem **24:**24-33.
30. **Olive PL, Chaplin DJ, Durand RE.** 1985. Pharmacokinetics, binding and distribution of Hoechst 33342 in spheroids and murine tumours. Br J Cancer **52:**739-746.
31. **Wang X-J, Chu N-Y, Wang Q-H, Liu C, Jiang C-g, Wang X-Y, Ikejima T, Cheng M-S.** 2012. Newly synthesized bis-benzimidazole derivatives exerting anti-tumor activity through induction of apoptosis and autophagy. Bioorganic & Medicinal Chemistry Letters **22:**6297-6300.
32. **Baraldi PG, Bovero A, Fruttarolo F, Preti D, Tabrizi MA, Pavani MG, Romagnoli R.** 2004. DNA minor groove binders as potential antitumor and antimicrobial agents. Med Res Rev **24:**475-528.
33. **Chen AY, Yu C, Bodley A, Peng LF, Liu LF.** 1993. A new mammalian DNA topoisomerase I poison Hoechst 33342: cytotoxicity and drug resistance in human cell cultures. Cancer Res **53:**1332-1337.
34. **Soderlind KJ, Gorodetsky B, Singh AK, Bachur NR, Miller GG, Lown JW.** 1999. Bis-benzimidazole anticancer agents: targeting human tumour helicases. Anticancer Drug Des **14:**19-36.
35. **Woynarowski JM, McHugh M, Sigmund RD, Beerman TA.** 1989. Modulation of topoisomerase II catalytic activity by DNA minor groove binding agents distamycin, Hoechst 33258, and 4',6-diamidine-2-phenylindole. Mol Pharmacol **35:**177-182.
36. **Latt SA, Stetten G, Juergens LA, Willard HF, Scher CD.** 1975. Recent developments in the detection of deoxyribonucleic acid synthesis by 33258 Hoechst fluorescence. J Histochem Cytochem **23:**493-505.
37. **Downs TR, Wilfinger WW.** 1983. Fluorometric quantification of DNA in cells and tissue. Analytical biochemistry **131:**538-547.
38. **Goracci L, Germani R, Savelli G, Bassani DM.** 2005. Hoechst 33258 as a pH-sensitive probe to study the interaction of amine oxide surfactants with DNA. Chembiochem **6:**197-203.
39. **Schabel Jr FM.** 1968. The Antiviral Activity of 9-β-D-Arabinofuranosyladenine (ARA-A). Chemotherapy **13:**321-338.
40. **Furth JJ, Cohen SS.** 1968. Inhibition of mammalian DNA polymerase by the 5'-triphosphate of 1-beta-d-arabinofuranosylcytosine and the 5'-triphosphate of 9-beta-d-arabinofuranoxyladenine. Cancer Res **28:**2061-2067.
41. **Yakimovich A, Andriasyan V, Witte R, Wang IH, Prasad V, Suomalainen M, Greber UF.** 2015. Plaque2.0-A High-Throughput Analysis Framework to Score Virus-Cell Transmission and Clonal Cell Expansion. PLoS One **10:**e0138760.
42. **Kilcher S, Mercer J.** 2015. DNA virus uncoating. Virology **479:**578-590.

43. **Yamauchi Y, Greber UF.** 2016. Principles of virus uncoating: cues and the snooker ball. Traffic **17:**569-592.
44. **Mercer J, Snijder B, Sacher R, Burkard C, Bleck CK, Stahlberg H, Pelkmans L, Helenius A.** 2012. RNAi screening reveals proteasome- and Cullin3-dependent stages in vaccinia virus infection. Cell Rep **2:**1036-1047.
45. **Welsch S, Doglio L, Schleich S, Krijnse Locker J.** 2003. The vaccinia virus I3L gene product is localized to a complex endoplasmic reticulum-associated structure that contains the viral parental DNA. J Virol **77:**6014-6028.
46. **Artenstein AW, Johnson C, Marbury TC, Morrison D, Blum PS, Kemp T, Nichols R, Balser JP, Currie M, Monath TP.** 2005. A novel, cell culture-derived smallpox vaccine in vaccinia-naive adults. Vaccine **23:**3301-3309.
47. **Kilcher S, Schmidt FI, Schneider C, Kopf M, Helenius A, Mercer J.** 2014. siRNA Screen of Early Poxvirus Genes Identifies the AAA+ ATPase D5 as the Virus Genome-Uncoating Factor. Cell host & microbe **15:**103-112.
48. **Wang I-H, Suomalainen M, Andriasyan V, Kilcher S, Mercer J, Neef A, Luedtke NW, Greber UF.** 2013. Tracking viral genomes in host cells at single-molecule resolution. Cell host & microbe **14:**468-480.
49. **Senkevich TG, Koonin EV, Moss B.** 2009. Predicted poxvirus FEN1-like nuclease required for homologous recombination, double-strand break repair and full-size genome formation. Proceedings of the National Academy of Sciences **106:**17921-17926.
50. **McInnes CJ, Wood AR, Nettleton PF, Gilray JA.** 2001. Genomic comparison of an avirulent strain of Orf virus with that of a virulent wild type isolate reveals that the Orf virus G2L gene is non-essential for replication. Virus Genes **22:**141-150.
51. **McInnes CJ, Wood AR, Thomas K, Sainsbury AW, Gurnell J, Dein FJ, Nettleton PF.** 2006. Genomic characterization of a novel poxvirus contributing to the decline of the red squirrel (Sciurus vulgaris) in the UK. Journal of General Virology **87:**2115-2125.
52. **Yakimovich A, Gumpert H, Burckhardt CJ, Lütschg VA, Jurgeit A, Sbalzarini IF, Greber UF.** 2012. Cell-free transmission of human adenovirus by passive mass transfer in cell culture simulated in a computer model. Journal of virology **86:**10123-10137.
53. **Flatt JW, Greber UF.** Viral mechanisms for docking and delivering at nuclear pore complexes, p. *In* (ed), Elsevier,
54. **Moss B.** 2007. Poxviridae: The Viruses and Their Replication. Fields Virology **5th Edition:**2905-2946.
55. **Cyrklaff M, Risco C, Fernandez JJ, Jimenez MV, Esteban M, Baumeister W, Carrascosa JL.** 2005. Cryo-electron tomography of vaccinia virus. Proc Natl Acad Sci U S A **102:**2772-2777.
56. **Dales S.** 1963. The uptake and development of vaccinia virus in strain L cells followed with labeled viral deoxyribonucleic acid. The Journal of cell biology **18:**51-72.
57. **Hollinshead M, Vanderplasschen A, Smith GL, Vaux DJ.** 1999. Vaccinia virus intracellular mature virions contain only one lipid membrane. Journal of virology **73:**1503-1517.
58. **Schmidt FI, Bleck CK, Reh L, Novy K, Wollscheid B, Helenius A, Stahlberg H, Mercer J.** 2013. Vaccinia virus entry is followed by core activation and proteasome-mediated release of the immunomodulatory effector VH1 from lateral bodies. Cell Rep **4:**464-476.
59. **Chang DK, Cheng SF.** 1996. On the importance of van der Waals interaction in the groove binding of DNA with ligands: restrained molecular dynamics study. Int J Biol Macromol **19:**279-285.
60. **Sauers RR.** 1995. An analysis of van der Waals attractive forces in DNA-minor groove binding. Bioorganic & Medicinal Chemistry Letters **5:**2573-2576.
61. **Hatcher EL, Wang C, Lefkowitz EJ.** 2015. Genome variability and gene content in chordopoxviruses: dependence on microsatellites. Viruses **7:**2126-2146.
62. **Flatt JW, Greber UF.** 2015. Misdelivery at the nuclear pore complex—stopping a virus dead in its tracks. Cells **4:**277-296.

63. **Kobiler O, Drayman N, Butin-Israeli V, Oppenheim A.** 2012. Virus strategies for passing the nuclear envelope barrier. Nucleus **3:**526-539.

64. **Puntener D, Greber UF.** DNA-tumor virus entry—From plasma membrane to the nucleus, p 631-642. *In* (ed), Elsevier,

65. **Smee DF, Sidwell RW, Kefauver D, Bray M, Huggins JW.** 2002. Characterization of wild-type and cidofovir-resistant strains of camelpox, cowpox, monkeypox, and vaccinia viruses. Antimicrob Agents Chemother **46:**1329-1335.

66. **Moss B.** 2013. Poxviridae, p 2664. *In* Fields BN, Knipe DM, Howley PM, Cohen IJ, Griffin DE, Lamb RA, A MM, R RV, B R (ed), Fields Virology, 6 ed, vol 1. Lippincott Williams & Wilkins, a Wolters Kluwer business, Philadelphia, USA.

67. **Sekiguchi J, Shuman S.** 1997. Mutational analysis of vaccinia virus topoisomerase identifies residues involved in DNA binding. Nucleic acids research **25:**3649-3656.

68. **Mutsafi Y, Fridmann-Sirkis Y, Milrot E, Hevroni L, Minsky A.** 2014. Infection cycles of large DNA viruses: emerging themes and underlying questions. Virology **466-467:**3-14.

69. **Patel SR, Kvols LK, Rubin J, O'Connell MJ, Edmonson JH, Ames MM, Kovach JS.** 1991. Phase I-II study of pibenzimol hydrochloride (NSC 322921) in advanced pancreatic carcinoma. Invest New Drugs **9:**53-57.

70. **Quenelle DC, Prichard MN, Keith KA, Hruby DE, Jordan R, Painter GR, Robertson A, Kern ER.** 2007. Synergistic efficacy of the combination of ST-246 with CMX001 against orthopoxviruses. Antimicrob Agents Chemother **51:**4118-4124.

71. **Mercer J, Helenius A.** 2008. Vaccinia virus uses macropinocytosis and apoptotic mimicry to enter host cells. Science **320:**531-535.

72. **Mercer J, Knebel S, Schmidt FI, Crouse J, Burkard C, Helenius A.** 2010. Vaccinia virus strains use distinct forms of macropinocytosis for host-cell entry. Proc Natl Acad Sci U S A **107:**9346-9351.

73. **Mercer J, Traktman P.** 2003. Investigation of structural and functional motifs within the vaccinia virus A14 phosphoprotein, an essential component of the virion membrane. Journal of virology **77:**8857-8871.

Figure Legends

Figure 1. (A) The chemical structure, properties including partitioning coefficient (LogP) and compound information of the bisbenzimides used in this study. (B) Bisbenzimides (H4, H5, H8) block VACV replication in tissue culture. BSC40 cells were infected with a serial dilution of E/L EGFP VACV and treated with serial dilutions of H4, H5, H8 or AraC. Full well images show EGFP expressing infected cells color-coded by intensity (left panels). Nuclei were detected by staining with Hoechst (right panels). Experiments were performed in triplicate and representative images displayed.

Figure 2. Quantification of infected EGFP expressing cells and total cell number (nuclei) from figure 1B. Grey bars indicate infection index and red boxes cell number for each condition tested. Experiments were performed in triplicate results displayed as mean ± SD.

Figure 3. Bisbenzimides inhibit VACV intermediate and late gene expression. (A and B) BSC40 (A) or HeLa (B) cells were infected with WR E EGFP (gray bars) or WR L EGFP (black bars) VACV. Cells were scored for EGFP expression by flow cytometry and infected cells quantified relative to untreated cells. CHX or AraC served as controls for these experiments. (C) HeLa cells treated with various concentrations of H4 were infected with WR E EGFP (blue line), or WR I EGFP (green line), or WR L EGFP (red line) and the percentage of EGFP-positive infected cells quantified by flow cytometry. These values were fitted to dose response curves to estimate EC_{50} and EC_{90} values (dashed lines).

Figure 4. H4 inhibits plaque formation, reduces virus yield, and blocks early VACV infection without impacting particle infectivity. (A) HeLa cells were infected with 150 pfu of WT VACV and infection allowed to proceed for 72h. The plates were stained with crystal violet to visualize plaques . (B) HeLa cells were infected with WT VACV (MOI 1). 24 hpi

cells were harvested, lysed and virus yield determined by titration and plaque formation. (C) HeLa cells were infected with WT virus (MOI 1) and 80nM H4 added at the indicated time points. A sample subjected to AraC addition at 6hpi was included as a positive control for inhibition. Cells were harvested 24 hpi and virus yield determined for each sample by serial dilution plaque assay. (D) HeLa cells were infected with WT virus (MOI 1) in the presence of 80nM H4. At the indicated time points, cells were washed and infection allowed to proceed. A sample subjected to AraC washout at 6hpi was included as a positive control for inhibition. At 24 hpi virus yield was determined for each sample by serial dilution plaque assay. (E) WR E EGFP (black bars) or WR L EGFP (white bars) virions were pre-incubated with 20nM or 80nM H4 for 30min at room temperature. Virus particles were washed three times and used to infect HeLa cells. Samples were analyzed by flow cytometry for infected EGFP-positive cells at 6 hpi (early) and 8 hpi (late). (F) WR E/L EGFP virions were pre-incubated with 2μM H4 for 2, 3 or 4 hours. Virions were washed and used to infect HeLa cells prior to fixation and analysis by plaque 2.0 for total nuclei and EGFP-positive infected cells. (A-F) All experiments were performed in triplicate and representative images shown (A) or results displayed as means ± SD (B-F).

Figure 5. H4 does not impact viral genome uncoating (A) HeLa cells were infected with WT VACV (MOI 10) in the presence of 20nM, 80nM or 200nM H4 and AraC. Pre-replication sites were visualized by immunofluorescence staining against I3 followed by confocal microscopy. CHX or AraC served as controls for uncoating and replication, respectively. (B) Quantification of pre-replication sites per cell from A. (A and B) Experiments were performed in triplicate, representative images displayed, and results displayed as mean ± SEM. Scale bar = 10 μm.

693 **Figure 6.** H4 attenuates VACV IG/LG transcription and DNA replication in a dose-
694 dependent fashion. (A) HeLa cells were infected (MOI 10) in the presence of 20nM, 80nM
695 or 200nM H4. At 8 hpi cells were fixed and stained with Dapi and imaged by confocal
696 microscopy. Scale bar = 10 μm. (B) The number of cells with cytoplasmic replication sites
697 was quantified per condition. AraC served as a control for inhibition of DNA replication site
698 formation. (C) HeLa cells were infected (MOI 10) in the presence of 20nM, 80nM or 200nM
699 H4 and EdU. At 8 hpi EdU incorporation was detected by Click-iT EdU Imaging kit followed
700 by confocal microscopy. Scale bar = 10 μm. (D) The total intensity of EdU incorporation
701 into replication sites was quantified and displayed as the mean ± SD. (E) The amount of
702 viral DNA from cells infected in the absence or presence of H4 at different concentrations
703 was quantified by qPCR at 8 hpi. AraC served as a control for inhibition of DNA replication
704 (F) The levels of early (J2), intermediate (G8), and late (F17) viral mRNA from infected
705 HeLa cells were quantified by RT-qPRC. Cells were infected in the absence of presence of
706 various concentrations of H4 and RT performed at 2 hpi for J2, 4 hpi for G8, and 8 hpi for
707 F17. Results are displayed as the average abundance normalized to untreated samples.
708 (A-D) All experiments were performed in triplicate and representative images (A and C) or
709 means ± SD (B, D-F) displayed.

710 **Figure 7.** Poxviruses are acutely sensitive to H4 inhibitory activity. (A) Foetal Lamb Skin
711 cell monolayers were infected with VACV or ORF-11 (100 pfu), MRI-SCAB (500 pfu), or
712 Squirrelpox (1000 pfu). Cells were fixed and plaques visualized by crystal violet staining at
713 3 days (VACV), 4 days (ORF-11), or 7 days (MRI-SCAB and SQPV). Experiments were
714 performed in triplicate and representative images shown (B) HeLa cells were infected with
715 EGFP-expressing variants of VACV WR, Herpes Simplex Virus 1 (HSV-1), Influenza A
716 virus (IAV), Vesicular Stomatitis Virus (VSV), or Semliki Forest Virus (SFV). For each,

infection was allowed to proceed for 6-8 h after which cells were analyzed for EGFP expression by flow cytometry. Experiments were performed in triplicate and the percent infection relative to untreated controls displayed as mean ± SD.

Figure 1

A

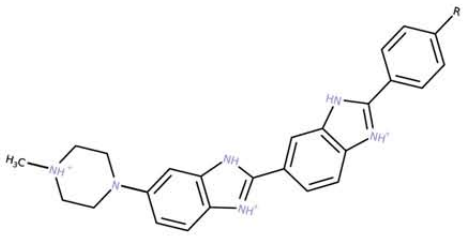

R-group	Hoechst Name	CAS Number	Short Name	Predicted LogP
$-CH_2CH_3$	33342	23491-52-3	H4	5.51
$-N(CH_3)_2$	33480	23555-00-2	H8	4.66
-OH	33258	23491-45-4	H5	4.25

B

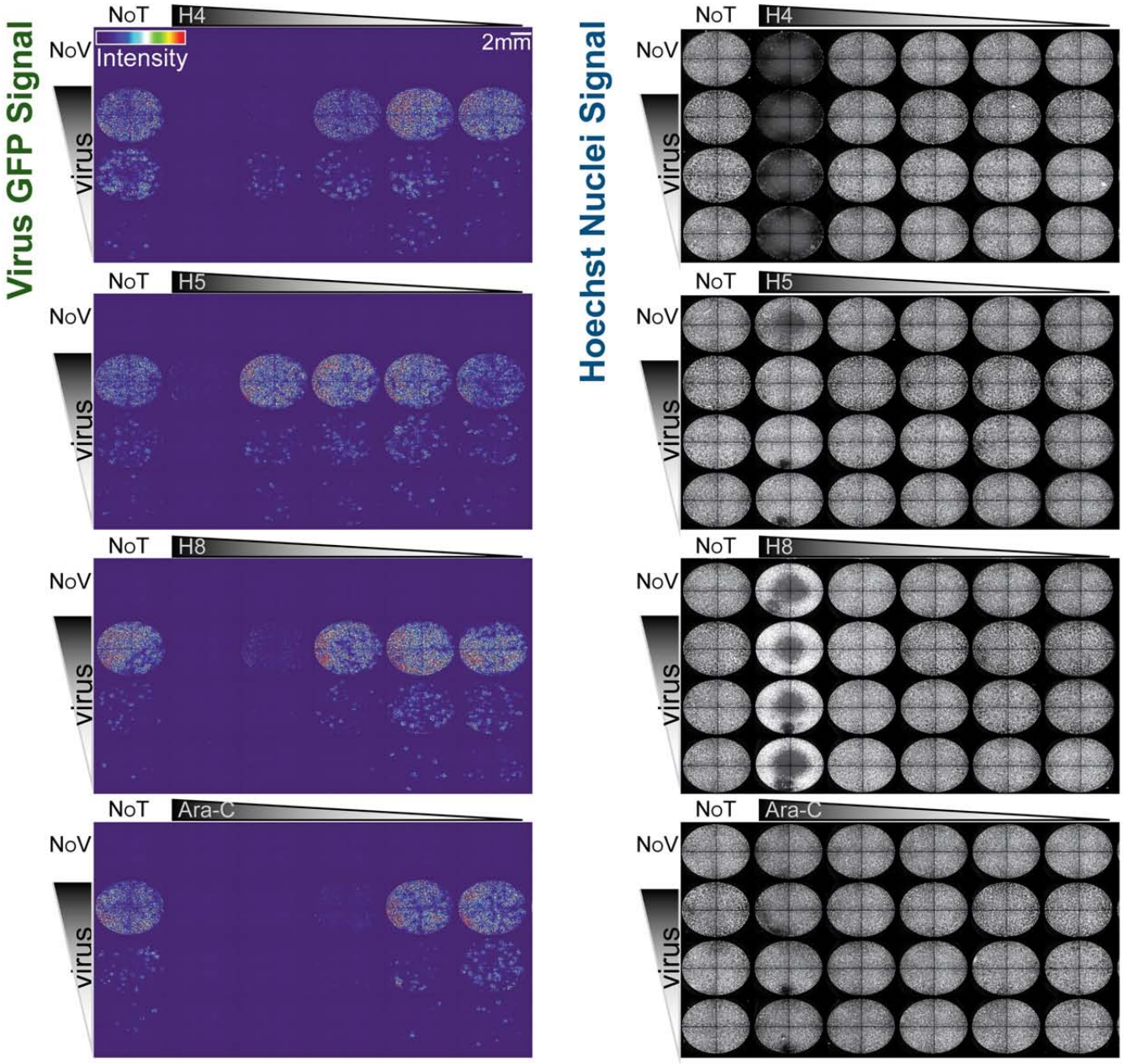

Figure 2

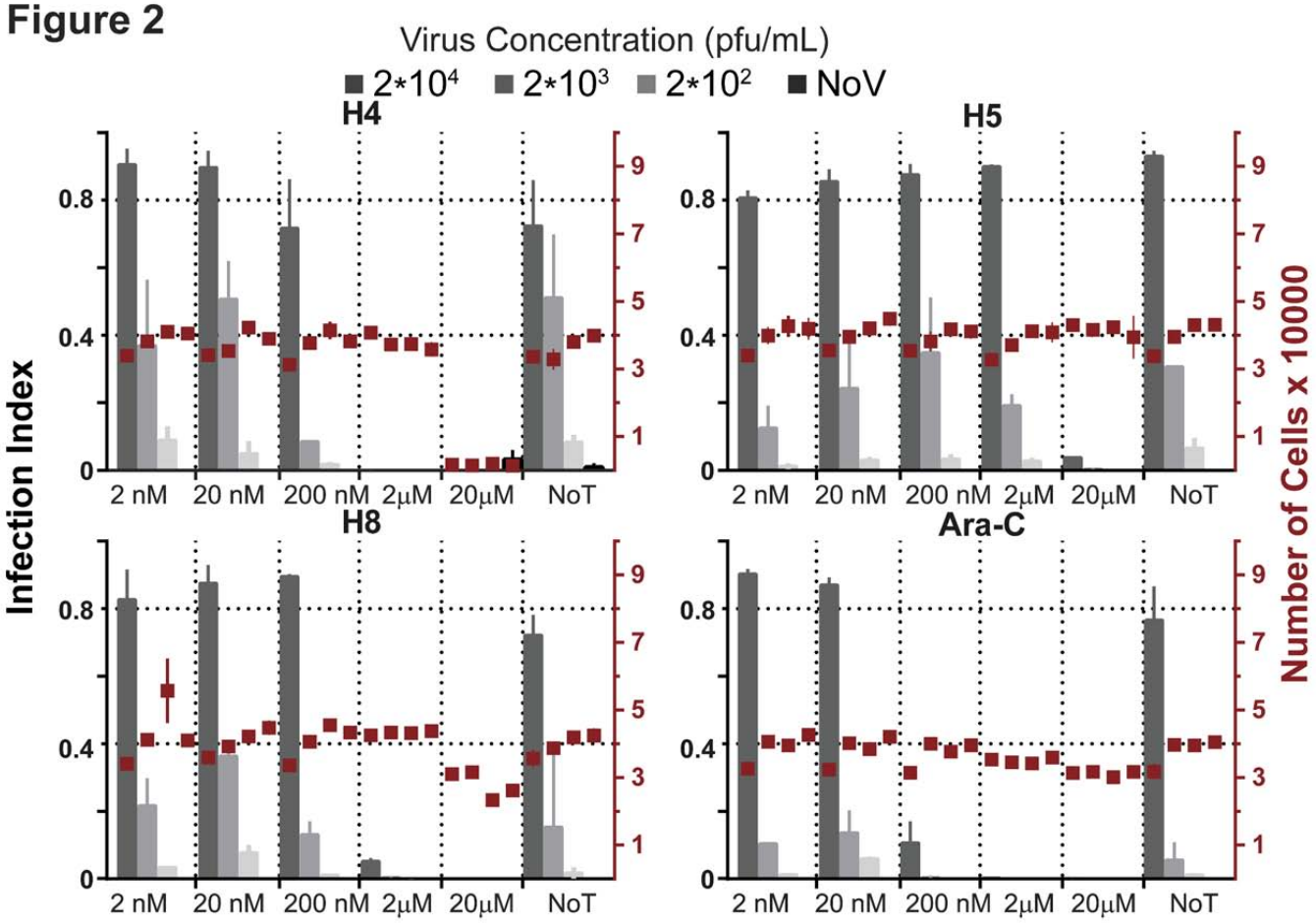

Figure 3

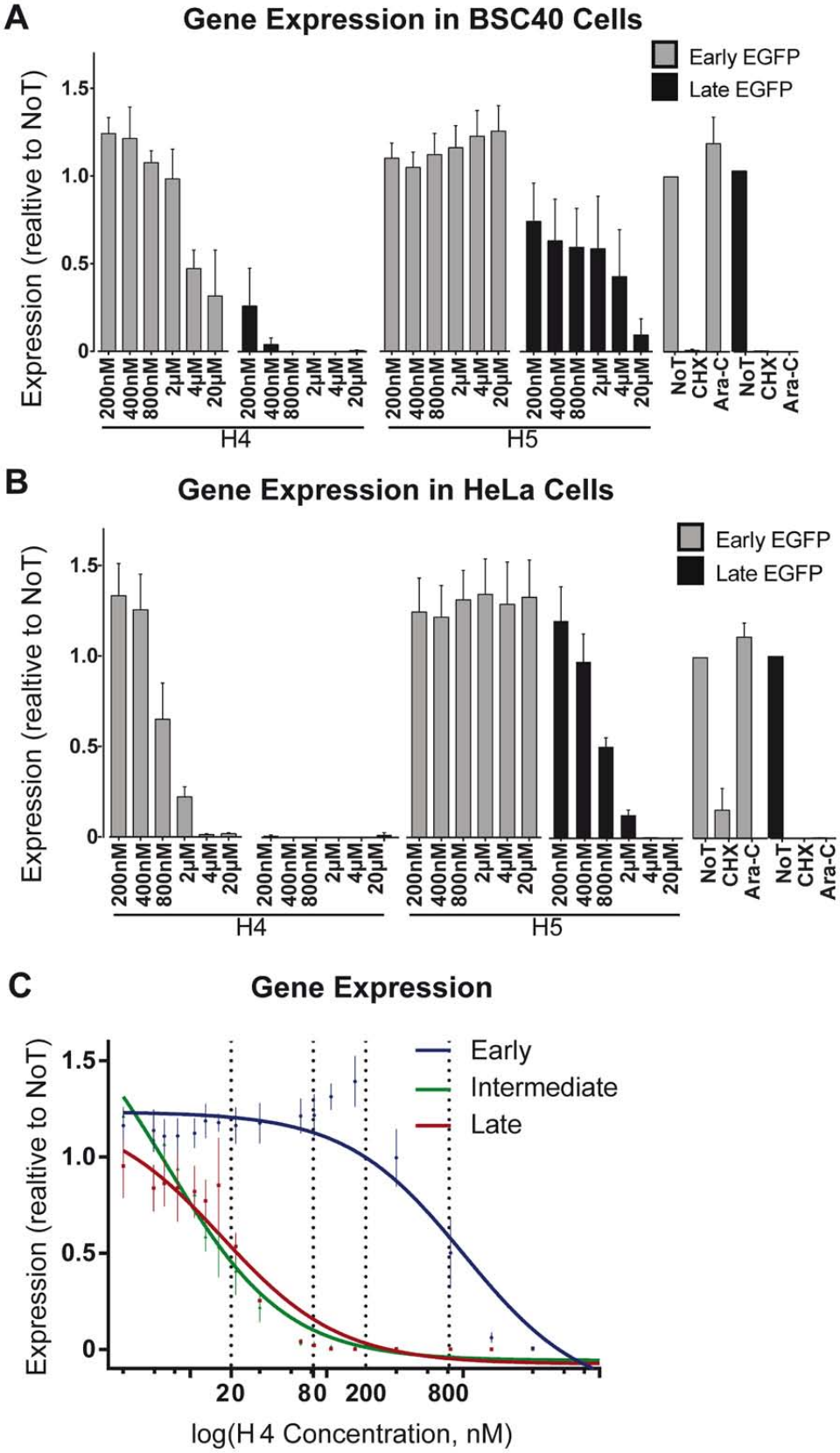

Figure 4

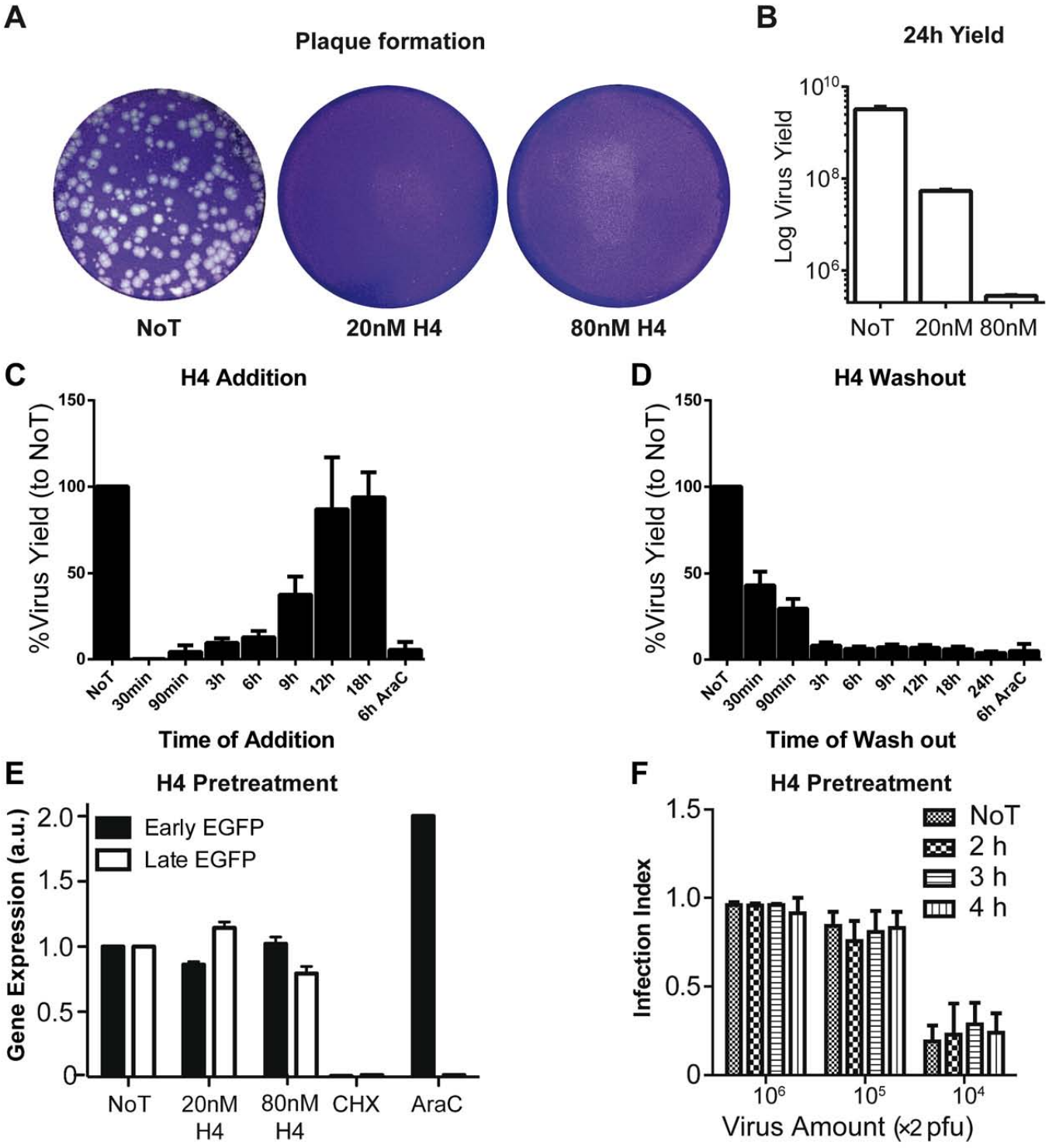

Figure 5

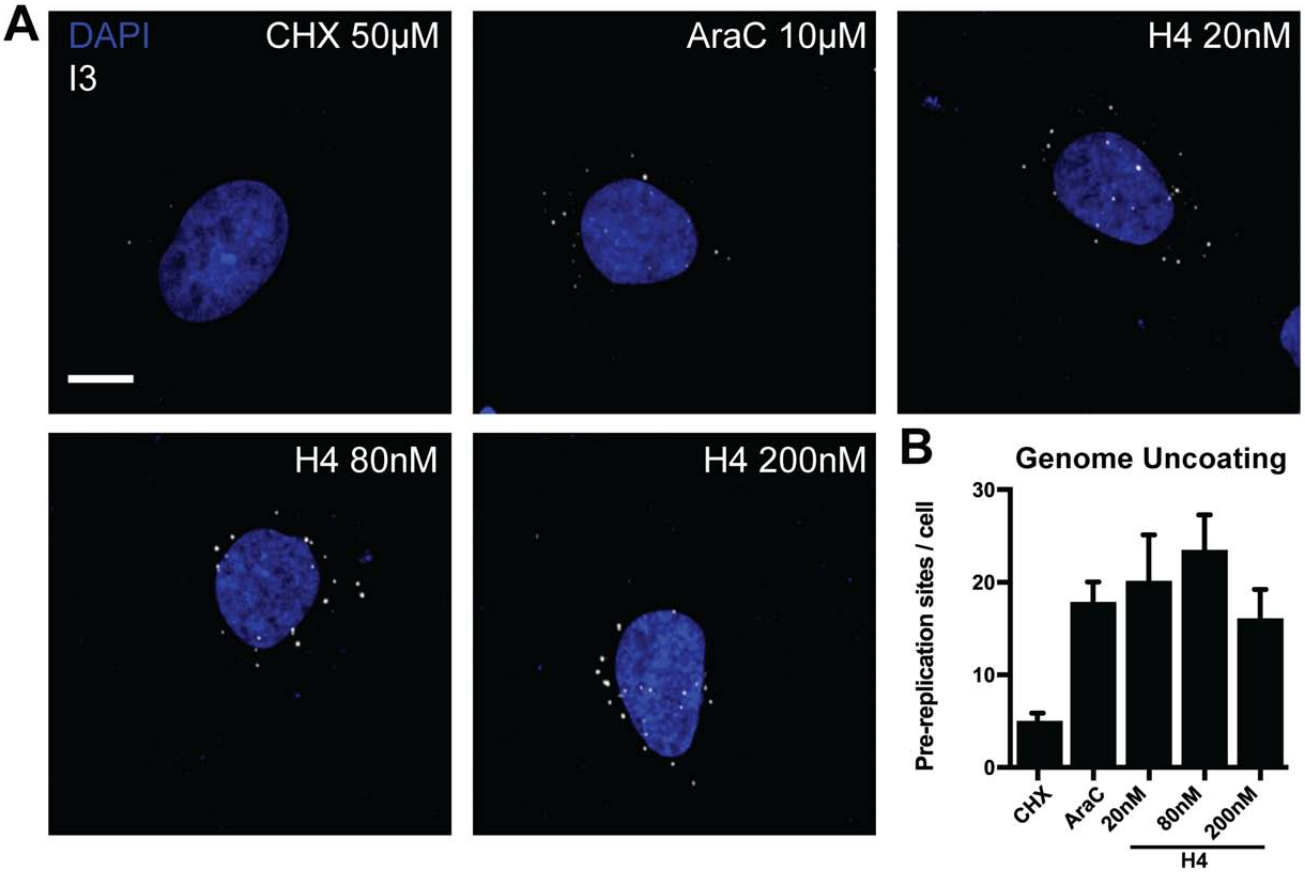

Figure 6

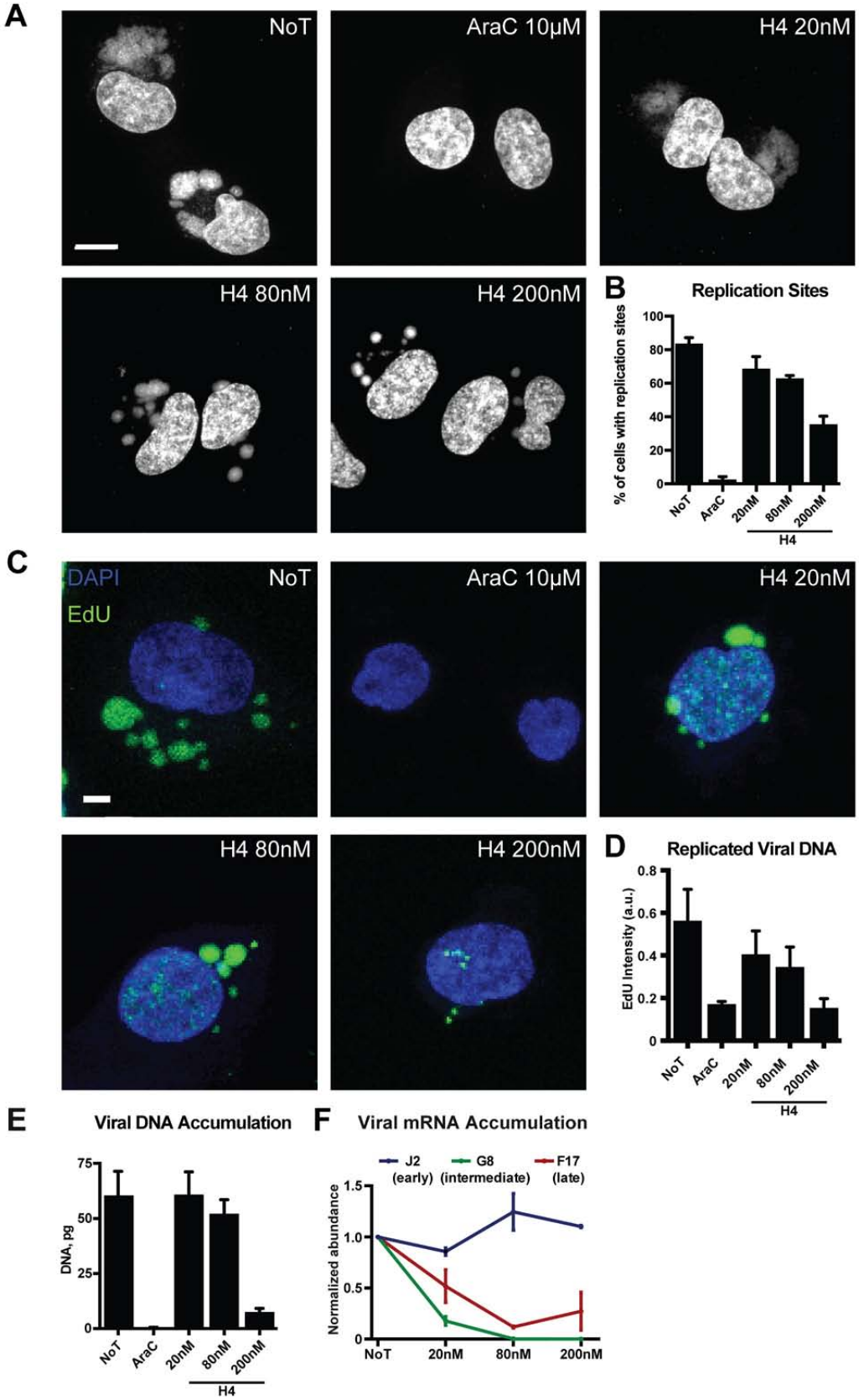

Figure 7